Analysis of Damage to Buildings in Urban Centers on Unstable Slopes via TerraSAR-X PSI Data: The Case Study of El Papiol Town (Spain)

D. Peduto, G. Nicodemo, M. Cuevas-Gonzáles, and M. Crosetto

***Abstract*— Persistent Scatterer Interferometry (PSI) data, deriving from the processing of SAR images acquired by high-resolution sensors such as TerraSAR-X, provide accurate measurements of displacements affecting structures (e.g., buildings) and linear infrastructure networks (e.g., roads, bridges, embankments, and pipelines). Such widespread displacements, when available on buildings on unstable slopes, offer new perspectives for their integration in procedures pursuing the analysis and the prediction of the physical vulnerability of exposed buildings. In this letter, both deterministic and probabilistic cause (differential settlements)—effects (damage) relationships are generated by using PSI-derived building settlements and the results of building damage surveys. The procedure is applied to El Papiol town (Spain), whose urban area has been suffering diffuse damage of different severity to buildings and roads due to extremely slow-moving landslide phenomena.**

***Index Terms*— Building damage, persistent scatterer interferometry (PSI) data, slow-moving landslides, TerraSAR-X, vulnerability.**

I. Introduction

SLOW-MOVING landslides yearly affect urban areas on hill slopes causing damage of different severity to the built-up heritage. This results in widespread increasing economic losses, unless appropriate risk mitigation strategies are set up. Within the landslide risk management framework [1], the assessment of vulnerability—which represents the expected degree of loss induced by an event of given intensity and return period—plays a key role, as it is testified by the growing interest of both scientific and technical communities. The building vulnerability assessment can be pursued following either numerical, or analytical, or empirical approaches [2]. The last ones, which are the most suitable for analyses at the municipal scale, require rich data sets collecting information on both landslides (e.g., displacing volume and kinematics) and exposed facilities (stiffness/strength of constituting materials, level of damage severity, maintenance state, and value) [1], [2].

Manuscript received December 6, 2018; revised February 13, 2019; accepted March 22, 2019. This work was supported by the Spanish Ministry of Economy and Competitiveness through the DEMOS project under Grant CGL2017-83704-P. *(Corresponding author: D. Peduto.)*

D. Peduto and G. Nicodemo are with the Department of Civil Engineering, University of Salerno, 84084 Fisciano (Salerno), Italy (e-mail: dpeduto@unisa.it; gnicodemo@unisa.it).

M. Cuevas-Gonzáles and M. Crosetto are with the Division of Geomatics, Centre Tecnològic de Telecomunicacions de Catalunya, E-08860 Barcelona, Spain (e-mail: mcuevas@cttc.cat; michele.crosetto@cttc.cat).

Color versions of one or more of the figures in this letter are available online at http://ieeexplore.ieee.org.

Digital Object Identifier 10.1109/LGRS.2019.2907557

Measurements of surface displacements derived from the processing of medium-/high-resolution SAR images via Persistent Scatterer Interferometry (PSI) techniques have been successfully applied for slow-moving landslide studies. In particular, the scientific literature is rich of examples mainly focusing on landslide characterization (i.e., detection, mapping, and definition of the state of activity) [3]–[8]. More recently, few authors started to investigate the behavior of single buildings located in landslide-affected areas [4], [9]–[13]. This was possible thanks to both the increased availability of high-resolution SAR sensor images that fit the specific requirements (in terms of resolution, density, and precision/accuracy) of analyses at the scale of single buildings and processing algorithms that provide high-quality information using PSI or SAR tomographic analyses [14], [15]. Such aspects may gain a growing interest in the next future, especially if one considers the limited sample of "real cases" of monitored buildings that the classic geotechnical damageability criteria [16]–[18] exploited to relate the selected parameters describing building foundation deformation with the associated effects in terms of damage level.

This letter aims to provide a further contribution to highlight the potential of PSI-derived building displacements resulting from processing high-resolution SAR sensor images in the analysis and forecast of building damage as a step in the vulnerability assessment of buildings interacting with slow-moving landslides. In particular, first deterministic empirical relationships are derived between settlements and the level of damage severity recorded by buildings in the urban area of El Papiol town (Spain). Then, via a probabilistic approach, all the uncertainties related to damage classification and building features are taken into account through the generation of fragility curves [9]–[13]. These latter, as it is shown in this letter, represent a promising tool for vulnerability analysis/forecast at the municipal scale, especially in view of the continuous efforts devoted by researchers for improving outputs (in terms of accuracy/precision, density of information) of PSI algorithms.

II. Methodology

The adopted methodology has been presented in [11] and applied on ENVISAT and COSMO-SkyMed data in [12]. This is a further case study concerning its application on TerraSAR-X data. It consists of three cascading phases (Fig. 1).

Phase I includes two subphases. In phase Ia, the landslide-exposed elements (i.e., buildings in this case) are identified

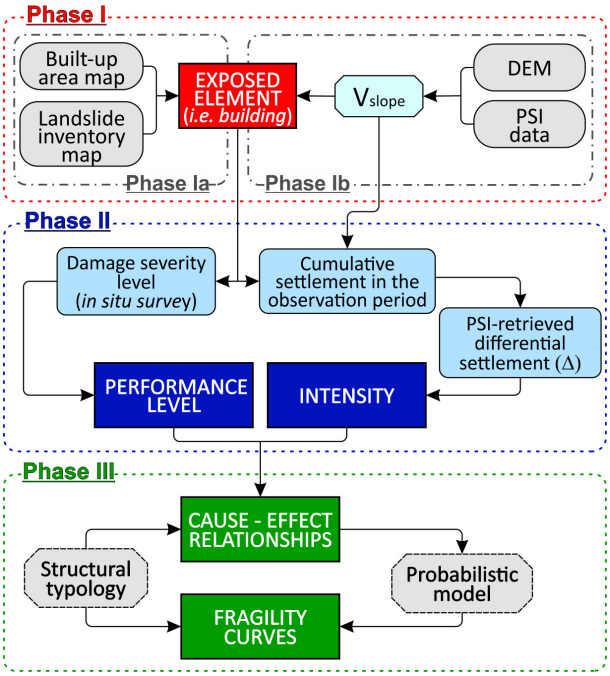

Fig. 1. Flowchart of the methodology.

by intersecting the maps of built-up area with the landslide inventory. In phase Ib, PSI data are converted according to [3] from the line-of-sight (LOS) sensor-target direction to the steepest slope direction, taking as input data a digital elevation model (DEM) of the area and the acquisition geometry of the sensor. Once the elements at risk are identified and the PSI velocities along the slope (V_{slope}) are computed, in phase II, a performance level (PL) as well as an intensity parameter are assigned to each exposed element. The former derives from the analysis of the building damage severity levels recorded during *in situ* surveys; the latter—assumed as the differential settlement (Δ) suffered from a given building—is calculated starting from the cumulative settlements derived by PSI data [11], [13], [19].

In phase III, buildings are homogenized based on their structural typology [e.g., reinforced concrete (R.C.) or masonry], which is one of the most relevant factors presiding over damage occurrence. In this last phase, end-products are twofold. First, cause (PSI-retrieved differential settlement, Δ)-effect (building damage expressed in terms of PL) relationships are retrieved. Then, empirical fragility curves, which provide the conditional probability P(•) for a randomly selected building at risk to be in, or exceed, a certain PL when the intensity parameter (Δ) equals a given value, are generated using the following equation [9]–[13]:

$$P(\text{Damage} \geq \text{PL}_i) = \phi\left[\frac{1}{\beta}\ln\left(\frac{\Delta}{\bar{\Delta}_i}\right)\right]. \quad (1)$$

To this aim, a log-normal distribution function $\phi[]$ is used as probabilistic model, wherein the fragility parameters (median $\bar{\Delta}_i$ and standard deviation β) are computed using the maximum likelihood method according to [20].

III. Study Area and Available Data Set

The study area consists of a portion of El Papiol (Catalunia, Spain) municipality [Fig. 2(a)]. It is a Mediterranean climate area with a historic center located in the upper part of the hill and a newly urbanized area developed in the 1960s, involving lands previously covered by agricultural fields. Both masonry buildings—mainly located in the historic center that includes a twelfth century castle—and R.C. ones—dating back to the major urbanistic expansion along the southern hill slope—compose the urban fabric. Starting from 1971 and mostly from 1983 on, following periods of heavy rainfall [8], part of the built-up area started exhibiting damages induced by ground instability. This led the El Papiol municipal government to set up a risk mitigation strategy including: 1) evacuation/repair ordinances for most affected buildings; 2) some control works to reduce the displacement rates; and 3) construction bans within the most affected-areas. A recent study [8], carried out by using geomorphological/geological criteria jointly with historical reports and PSI data, confirmed the instability of the area [Fig. 2(a)]. In particular, the authors highlighted the presence of cohesive soils with high clay content affected by soil creep [21] in correspondence of an alteration band of detrital material of Miocene Epoch at about 5 m depth. This phenomenon is characterized by extremely slow displacements that affect the built-up area [8]. The analysis of PSI time-series allowed for a more accurate definition of landslide boundaries [Fig. 2(a)]. PSI data were derived by processing 42 ascending StripMap TerraSAR-X SAR images using the PSIG approach described in [22]. The images are uniformly distributed over the observation period (December 2007 to June 2012) with perpendicular baselines that range from $-$ 333 to $+$ 506 m. The PSI spatial distribution of the velocity (i.e., the average value over the observation period) along the LOS (V_{LOS}) is shown in Fig. 2(a).

IV. Results

In Phase I, V_{LOS} values were converted to V_{slope}, also filtering out those PSs for which the multiplying factor between V_{slope} and V_{LOS} exceeded the threshold of 4 as suggested by [3], [4]. This operation was necessary to account for the constraints related to the geometry of both the sensor acquisition and the landslide-affected slope (e.g., 1-D LOS information leading to possible misinterpretations on both modulus and orientation of the "real" displacement vector when only one orbit data set is available; very limited sensitivity to northward/southward displacements, see among others [3] and [4]). The derived V_{slope} map of the El Papiol area is shown in Fig. 2(b).

As for the damage to the built-up area, in order to gather an overview of its severity and distribution within the entire urban area, an *in situ* expeditious damage survey was carried out in June–July 2017.

To this aim, the crack patterns exhibited by building façades were investigated and fact-sheets [10], [23] were filled in (Fig. 3). These documents contain information concerning the location and the urban fabric characteristics (e.g., structural type, foundation typology, number of floors, and occupancy type), a photo-collection regarding the damage recorded including the state of maintenance and assigned damage severity (classified in six levels: D0 = negligible; D1 = very

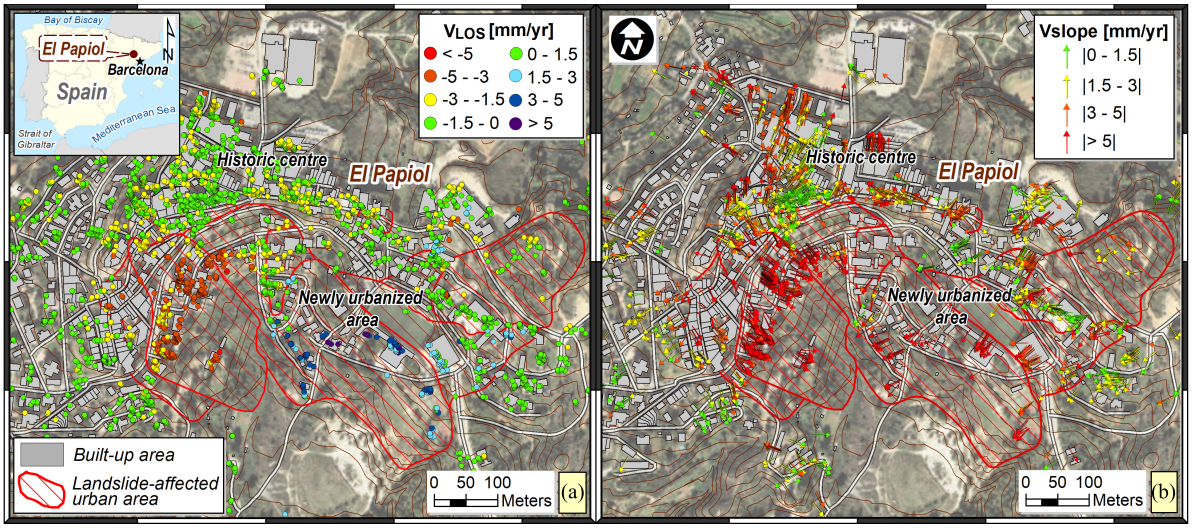

Fig. 2. El Papiol (Spain) study area. (a) Slow-moving landslide-affected urban area with spatial distribution of PSI V_{LOS} derived from the processing of 42 TerraSAR-X images acquired in StripMap mode on ascending orbit (December 2007 to June 2012). (b) PSI V_{slope} map.

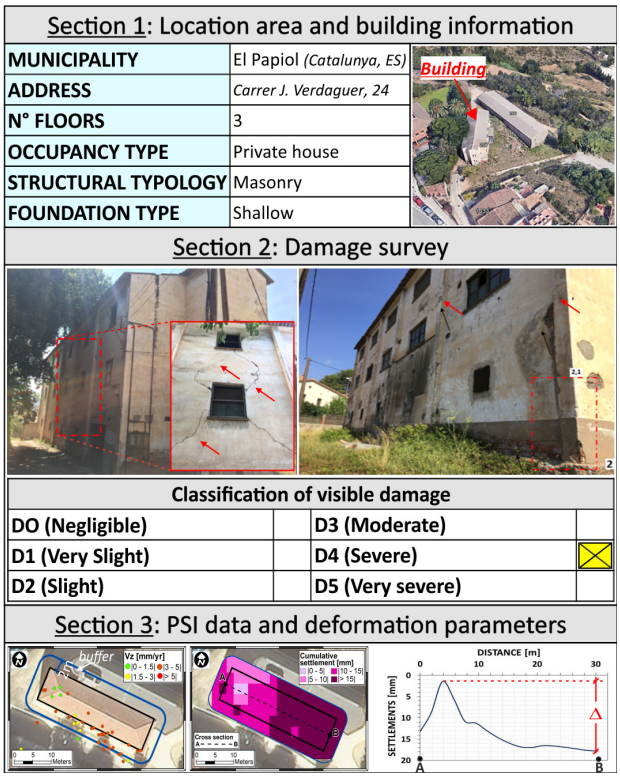

Fig. 3. Building fact-sheet: (Section I) location area and building information; (Section II) damage level and photographs of the field survey; (Section III) DInSAR data and retrieved deformation parameter (i.e., differential settlement, Δ).

slight; D2 = slight; D3 = moderate; D4 = severe; and D5 = very severe), the available PSI measurements, and derived foundation deformation parameter. In particular, during *in situ* surveys the level of damage was classified according to [24] based on the width and the diffusion of cracks on façades, and on their easy of repair.

The results of the survey campaign on 423 buildings are summarized in Fig. 4, in which the recorded damage severity

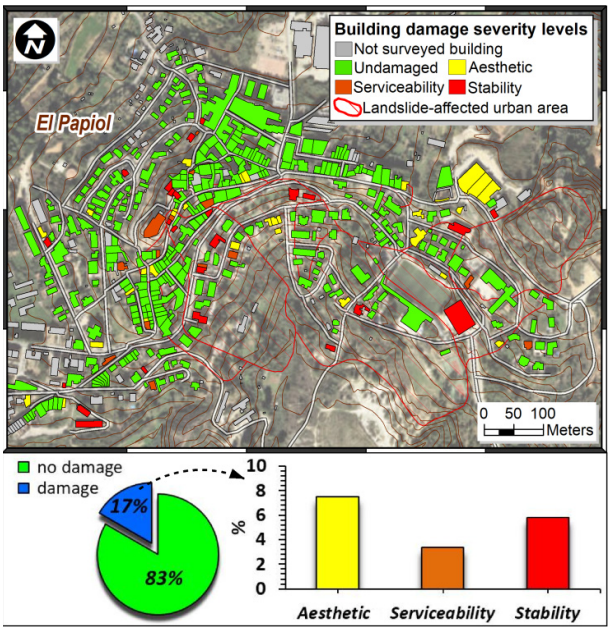

Fig. 4. Building damage map of El Papiol urban area.

levels were merged based on the building PL. For this purpose, four building PLs were considered: undamaged (when the building does not exhibit damage or only a negligible level D0 is recorded); esthetic (including D1 and D2 damage levels characterized by hairline/fine cracks that can be easily treated during normal decoration or require easy repair works); serviceability (associated with D3 severity level, where moderate damages that need maintenance works are recorded); stability (referred to D4 and D5 damage severity levels with a risk for building safety because the damage can affect its structural stability).

The collected data highlight that 83% out of the total surveyed buildings do not exhibit damage. As for the remaining 17% ones, they exhibit severity levels classified as aestethic (7.5%), serviceability (3.5%), and stability (6%). The

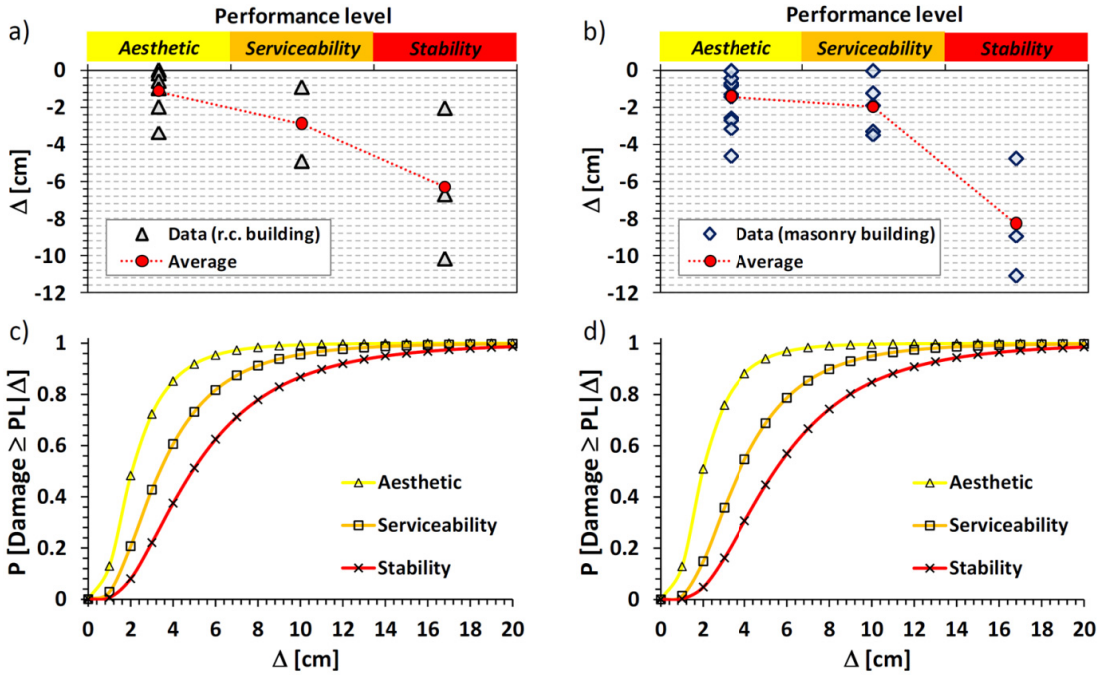

Fig. 5. PL versus differential settlements Δ for (a) R.C. and (b) masonry buildings in El Papiol urban area. Empirical fragility curves for (c) R.C. and (d) masonry buildings.

damaged buildings mainly concentrate on landslide-affected areas or in their proximity (Fig. 4), where the landslide mechanism is enlarging or retrogressing. For the purpose of the analysis, according to the available data, 34 buildings were identified as the exposed elements within landslide boundaries and covered by at least two coherent PSs. They were then distinguished based on their structural typology (22 masonry buildings and 12 reinforced ones).

In Phase II, each exposed building was associated with both a PL and a value of the intensity parameter (i.e., differential settlement Δ), computed as shown in Fig. 3. In particular, each building was associated with the PSs falling within a 2-m buffer around its perimeter and exhibiting height comparable to that of the building. Then, the cumulative settlement pertaining to each PS was derived by multiplying the vertical component (V_z) of V_{slope} by the reference period of 34 years (i.e., the time passed between the major event of 1983, when damage started being recorded, and the date of the damage survey in 2017). In this way, a constant velocity (i.e., the one computed during PSI observation period) was assumed over 34 years. This assumption, although creep evolving with extremely slow velocity is considered the cause of the slope instabilities in El Papiol area [8], represents a current limit to this letter.

PS-derived settlement data were then interpolated via inverse distance weight (IDW) method on a 2 by 2 m grid over each building, so that settlement profiles were retrieved along the longitudinal cross sections. Then, the differential settlement Δ was computed as the maximum difference of the vertical settlement between any two points along the settlement profile of the single building's foundation (Fig. 3). In this way, although settlements refer to PS located on the building roof, they were considered as occurring at the foundation level, thus neglecting either compressive or tensile strains that may affect the superstructure [11] as well as possible thermal expansion of materials [25], [26].

TABLE I

MEDIAN ($\bar{\Delta}_i$) AND STANDARD DEVIATION (β) PARAMETERS OF THE LOG-NORMAL DISTRIBUTION FUNCTION USED FOR EACH CONSIDERED PL

Performance level	Building typology			
	R.C.		Masonry	
	$\bar{\Delta}_i$ [cm]	β[cm]	$\bar{\Delta}_i$ [cm]	β[cm]
Aesthetic	2.06		1.97	
Serviceability	3.37	0.64	3.73	0.59
Stability	4.90		5.41	

In Phase III, empirical relationships were derived between Δ and the PL for the samples of R.C. [Fig. 5(a)] and masonry buildings [Fig. 5(b)]. For both building structural typologies, an increase of building damage corresponding to an increase of the intensity parameter can be appreciated. On the other hand, a lower PL is recorded by the building when the value of the intensity parameter (Δ) increases. The obtained values of Δ pertaining to the attainment of instability conditions are comparable to those available in the scientific literature, see for instance [16].

Finally, two sets of fragility curves [Fig. 5(c) and (d)] were computed relating Δ and the probability of attaining or exceeding one of the three PLs. Table I shows median ($\bar{\Delta}_i$) and standard deviation (β) parameters of the log-normal distribution function used for each considered PL derived by adopting the maximum likelihood estimation method according to [20].

V. Conclusion

In this letter, the potential of high-resolution TerraSAR-X PSI data in the analysis of vulnerability of buildings located in slow-moving landslide-affected areas was shown. For the case study of El Papiol town (Spain), by combining PSI-derived building differential settlements with the results of an expeditious *in situ* damage survey, it was possible to retrieve deterministic relationships between the level of damage severity and the values of the intensity parameter Δ cumulated over a period corresponding to the time interval between the last major reactivation event and the damage survey. As expected, higher values of Δ correspond to higher levels of damage severity for both the sample of reinforced and masonry buildings analyzed. The same data set was then used to generate probabilistic tools such as empirical fragility curves. These latter, whether a larger damaged building data set is available, could help appreciating the performance of different structural typologies. Indeed, so forth main limit to the diffusion of these tools has been the availability of settlement data from conventional monitoring techniques, which can turn out to be not affordable for analyses over large urban areas. Once further validated, fragility curves could stand as operative tools allowing for the prioritization of interventions and maintenance works to the exposed buildings that exhibit/may exhibit the lowest PL (or the highest damage severity) within an urban area.

Together with the research works carried out in the last decades for the application of PSI data for landslide mapping and characterization, the analysis of vulnerability of exposed elements could represent a further step toward the full integration of PSI data within the landslide risk management.

Acknowledgment

This work was carried out within an Erasmus for Traineeship Agreement between the Group of Geotechnical Engineering of Salerno University and CTTC/CERCA. This agreement allowed Valerio Parrella to carry out his M.Sc. thesis activities that contributed to the research.

References

[1] R. Fell, J. Corominas, C. Bonnard, L. Cascini, E. Leroi, and W. Z. Savage, "Guidelines for landslide susceptibility, hazard and risk zoning for land-use planning," *Eng. Geol.*, vol. 102, nos. 3–4, pp. 99–111, Dec. 2008.

[2] O. Mavrouli *et al.*, "Vulnerability assessment for reinforced concrete buildings exposed to landslides," *Bull. Eng. Geol. Environ.*, vol. 73, no. 2, pp. 265–289, May 2014.

[3] L. Cascini, G. Fornaro, and D. Peduto, "Advanced low- and full-resolution DInSAR map generation for slow-moving landslide analysis at different scales," *Eng. Geol.*, vol. 112, nos. 1–4, pp. 29–42, Mar. 2010.

[4] L. Cascini, D. Peduto, G. Pisciotta, L. Arena, S. Ferlisi, and G. Fornaro, "The combination of DInSAR and facility damage data for the updating of slow-moving landslide inventory maps at medium scale," *Natural Hazards Earth Syst. Sci.*, vol. 13, no. 6, pp. 1527–1549, Jun. 2013.

[5] F. Cigna, S. Bianchini, and N. Casagli, "How to assess landslide activity and intensity with persistent scatterer interferometry (PSI): The PSI-based matrix approach," *Landslides*, vol. 10, no. 3, pp. 267–283, Jun. 2013.

[6] M. Crosetto, O. Monserrat, M. Cuevas-González, N. Devanthéry, and B. Crippa, "Persistent Scatterer interferometry: A review," *ISPRS J. Photogramm. Remote Sens.*, vol. 115, pp. 78–89, May 2016.

[7] G. Gullà, D. Peduto, L. Borrelli, L. Antronico, and G. Fornaro, "Geometric and kinematic characterization of landslides affecting urban areas: The Lungro case study (Calabria, Southern Italy)," *Landslides*, vol. 14, no. 1, pp. 171–188, Feb. 2017.

[8] M. Crosetto, R. Copons, M. Cuevas-González, N. Devanthéry, and O. Monserrat, "Monitoring soil creep landsliding in an urban area using persistent scatterer interferometry (El Papiol, Catalonia, Spain)," *Landslides*, vol. 15, no. 7, pp. 1317–1329, Jul. 2018.

[9] D. Peduto *et al.*, "A procedure for the analysis of building vulnerability to slow-moving landslides," in *Proc. 1st IMEKO TC4 Int. Workshop Metrol. Geotech.*, Benevento, Italy, Mar. 2016, pp. 248–254.

[10] G. Nicodemo *et al.*, "Analysis of building vulnerability to slow-moving landslides via A-DInSAR and damage survey data," in *Proc. 4th WLF Landslide Forum*. Ljubljana, Slovenia: Springer, May/Jun. 2017, pp. 889–907. doi: 10.1007/978-3-319-53498-5_102.

[11] D. Peduto, S. Ferlisi, G. Nicodemo, D. Reale, G. Pisciotta, and G. Gullà, "Empirical fragility and vulnerability curves for buildings exposed to slow-moving landslides at medium and large scales," *Landslides*, vol. 14, no. 6, pp. 1993–2007, Dec. 2017.

[12] G. Nicodemo, D. Peduto, S. Ferlisi, G. Gullà, D. Reale, and G. Fornaro, "Dinsar data integration in vulnerability analyses of buildings exposed to slow-moving landslides," in *Proc. IEEE Int. Geosci. Remote Sens. Symp. (IGARSS)*, Valencia, Spain, Jul. 2018, pp. 6111–6114. [Online]. Available: https://ieeexplore.ieee.org/document/8518808

[13] D. Peduto, G. Nicodemo, M. Caraffa, and G. Gullà, "Quantitative analysis of consequences to masonry buildings interacting with slow-moving landslide mechanisms: A case study," *Landslides*, vol. 15, no. 10, pp. 2017–2030, Oct. 2018.

[14] X. Zhu and R. Bamler, "Very high resolution spaceborne SAR tomography in urban environment," *IEEE Trans. Geosci. Remote Sens.*, vol. 48, no. 12, pp. 4296–4308, Dec. 2010.

[15] G. Fornaro, F. Lombardini, A. Pauciullo, D. Reale, and F. Viviani, "Tomographic processing of interferometric SAR data: Developments, applications, and future research perspectives," *IEEE Signal Process. Mag.*, vol. 31, no. 4, pp. 41–50, Jul. 2014.

[16] A. W. Skempton and D. H. MacDonald, "The allowable settlements of buildings," in *Proc. ICE (Inst. Civil Eng.)*, vol. 5, 1956, pp. 727–768.

[17] R. Grant, J. T. Christian, and E. H. Vanmarcke, "Differential settlement of buildings," *J. Geotech. Eng. Division*, vol. 100, no. 9, pp. 973–991, 1974.

[18] J. B. Burland and C. P. Wroth, "Settlement of buildings and associated damage," in *Proc. Conf. Settl. Struct.*, Pentech, London, 1974, pp. 611–654.

[19] G. Nicodemo, D. Peduto, S. Ferlisi, and J. Maccabiani, "Investigating building settlements via very high resolution SAR sensors," in *Proc. IALCCE*. Delft, The Netherlands: Taylor & Francis, Oct. 2016, pp. 2256–2263.

[20] M. Shinozuka, M. Q. Feng, H. K. Kim, T. Uzawa, and T. Ueda, "Statistical analysis of fragility curves," State Univ. New York Syst., Buffalo, NY, USA, Tech. Rep. MCEER-03-0002, 2003.

[21] O. Hungr, S. Leroueil, and L. Picarelli, "The Varnes classification of landslide types, an update," *Landslides*, vol. 11, no. 2, pp. 167–194, Apr. 2014.

[22] N. Devanthéry, M. Crosetto, O. Monserrat, M. Cuevas-González, and B. Crippa, "An approach to persistent scatterer interferometry," *Remote Sens.*, vol. 6, no. 7, pp. 6662–6679, Jul. 2014.

[23] S. Ferlisi, D. Peduto, G. Gullà, G. Nicodemo, L. Borrelli, and G. Fornaro, "The use of DInSAR data for the analysis of building damage induced by slow-moving landslides," in *Proc. Eng. Geol. Soc. Territory*, vol. 2. Cham, Switzerland: Springer, 2015, pp. 1835–1839.

[24] J. B. Burland, B. B. Broms, and V. F. B. de Mello, "Behaviour of foundations and structures," in *Proc. 9th Int. Conf. SMFE, SOA Rep.*, Tokyo, Japan, vol. 2, 1977, pp. 495–546.

[25] F. Weissgerber, E. Colin-Koeniguer, J.-M. Nicolas, and N. Trouvé, "3D monitoring of buildings using TerraSAR-X InSAR, DInSAR and PolSAR capacities," *Remote Sens.*, vol. 9, no. 10, p. 1010, 2017. doi: 10.3390/rs9101010.

[26] G. Fornaro, D. Reale, and S. Verde, "Bridge thermal dilation monitoring with millimeter sensitivity via multidimensional SAR imaging," *IEEE Geosci. Remote Sens. Lett.*, vol. 10, no. 4, pp. 677–681, Jul. 2013.